MI-0057

A TRANSITIONLESS LATTICE FOR THE FERMILAB MAIN INJECTOR

K.Y. NG, D. TRBOJEVIC, S.Y. LEE

A Transitionless Lattice for the Fermilab Main Injector

K.Y. Ng, D. Trbojevic
*Fermi National Accelerator Laboratory,*P.O. Box 500, Batavia, IL 60510*
S.Y. Lee
Physics Department, Indiana University, Bloomington, IN 47405

Abstract

Medium energy (1 to 30 GeV) accelerators are often confronted with transition crossing during acceleration. A lattice without transition is presented, which is a design for the Fermilab Main Injector. The main properties of this lattice are that the γ_t is an imaginary number, the maxima of the dispersion function are small, and two long-straight section with zero dispersion.

I. Introduction

Most medium energy proton accelerators exhibit transition between injection and the end of the acceleration cycles. There are many unfavorable effects which can occur during and after transition[1]. For example, the momentum spread of a bunch around transition can become so large that it exceeds the machine momentum aperture and beam loss occurs[2]. There is little or no Landau damping against microwave instability near transition. As a result, the bunch area grows due to internal space-charge force as well as external beam-pipe wake forces. Particles with different momenta cross transition at different times leading to longitudinal distortions as well. The transition gamma for a particle with momentum p is defined as $1/\gamma_t^2 = (dC/C)/(dp/p)$, where C is the total path length of the particle around the accelerator. One way to avoid transition is to make $1/\gamma_t^2$ less than zero; or $dC/(dp/p) = \sum_i D_i\theta_i \leq 0$, where θ_i is the bending angle of the dipole at the position i, while D_i is the dispersion at the same location[3]. In Sect. II, the design method of such a lattice is reviewed. In Sect. III, a design for the Fermilab Main Injector is presented. We call this design an "advanced" γ_t lattice because it has a better compaction factor with respect to the one previously presented[4]. In Section IV, the chromaticities of the lattice are discussed and the dependence on momentum is analyzed. The tunability of the lattice, the betatron function and the tune dependence on the gradient errors in the main quadrupoles, the misalignment errors, as well as the study of the dynamical aperture will be given in a separate paper[5].

II. Review of the Design Method

The horizontal dispersion function is presented in a normalized Floquet's coordinate system as $\xi = D/\sqrt{\beta} = A\sin\phi$ and $\chi = D'\sqrt{\beta} + \alpha D/\sqrt{\beta} = A\cos\phi$, where D and D' are the dispersion and the slope of the dispersion function, respectively, while β , α, and ϕ are the Twiss parameters[6]. To provide an average negative value of the horizontal dispersion through the dipoles, most dipoles should be placed in a lattice with negative dispersion (within the third and fourth quadrants of the χ-ξ space.) The basic block of the imaginary γ_t lattice is presented in the normalized dispersion space in Fig. 1.

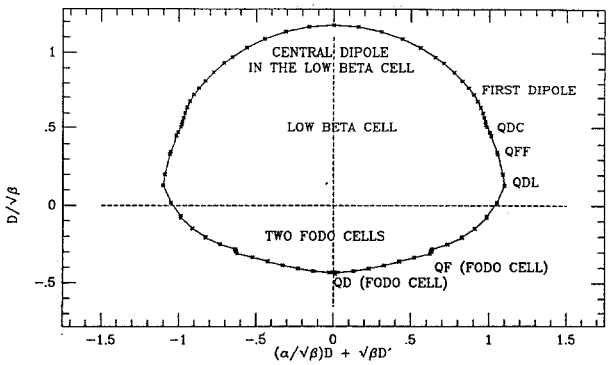

Fig. 1. *Normalized horizontal dispersion function in the basic block of the imaginary γ_t lattice.*

The second-order inhomogenious differential equation of motion can be represented as propagation of the betatron phase along a circle without changing the amplitude A for particle motion throughout all elements except the dipoles. In the thin element approximation, the motion through a dipole is presented by a vector parallel to the χ-axis with a length equal to $\Delta\chi \cong \theta\sqrt{\beta}$. When the dipole is thick, a change in the coordinate χ becomes a smooth curved function because of the phase advance through the dipole. As an approximation, the kick in the slope of the dispersion function is placed at the center of the dipole and the phase advance is taken into account from the dipole beginning to the center and from the center to the other end of the dipole. This method provides a very intuitive approach to the lattice design. The motion of a particle through the two FODO cells (12 dipoles—3 per half cell) is presented in the third and the fourth quadrants of the normalized space in Fig. 1. The second part of the normalized dispersion function plot, located mostly in the first and second quadrant of the ξ-χ space, represents a motion through the low-beta insertion cell. The major role of this cell is to provide the phase difference necessary to close the betatron functions, including the dispersion function to the beginning of the FODO cell. The low-beta insertion is symmetric and is defined with two quadrupole triplets. For compactness, the first D-quad of the first triplet replaces the last D-quad in the FODO cell which was present in the previous design. Although there are three dipoles in the middle of the low beta insertion cell, their influence on the dispersion function is very small due to the small values of β_x in this region. As a result, horizontal kicks can hardly be seen in the low-beta region in Fig. 1.

*Operated by the Universities Research Association under contract with the U.S. Department of Energy.

III. Lattice Properties

The design of the imaginary γ_t lattice in this example represents a possible solution for the 150 GeV future Main Injector in Fermilab. The transition gamma is an imaginary number, $\gamma_t = i24.37$. The lattice has to follow many geometrical constraints due to the limited site space. It also has to follow the shape of the tunnel of the existing FODO-cell-based design. There are 302 dipoles available; 8 straight sections at specific locations (two of which need to have zero dispersion), and the total length has to be exactly 3319.4186 meters.

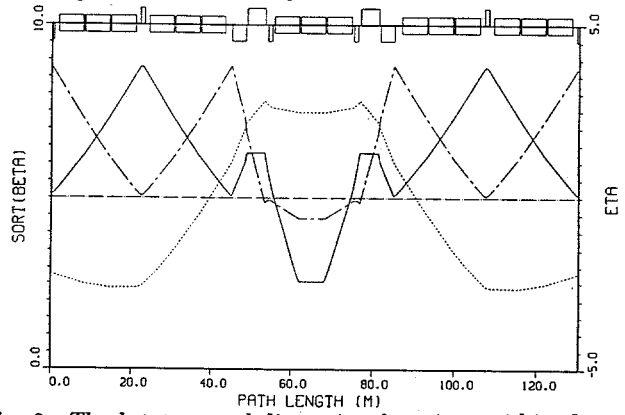

Fig. 2. *The betatron and dispersion functions within the regular block (BLR) of the imaginary γ_t lattice. The long-straight section block (BLS) is very similar, just with the 3rd, 4th, 7th, 8th, 9th, 12th, and 13th dipoles removed.*

The whole ring consists of three types of blocks. The basic block "*BLR*" (Fig. 2) consists of two 60° FODO cells containing 12 dipoles and a low-beta insertion containing 3 dipoles. The gradient of every quadrupole in the ring is ±220 kG/m. The maximum values of the horizontal and vertical betatron functions in the FODO cell are 77.42 m and 76.78 m, respectively. The quad lengths are 1.0325 m while the dipole length is defined as 6.096 m by the prototype magnet already built. The maximum and minimum of the dispersion function within the whole ring are −2.77 meters and +2.82 meters. Two FODO cells in a row are connected to the low-beta insertion where both betatron functions have minimum values in the center [$(\beta_x)_{\min} = 4.3$ m]. The low-beta insertion is defined with two triplets. The first quad of length 3.34 m in the triplet replaces the last quadrupole of the FODO cell which was present in the previous design. The central quad in the triplet has the longest length of 4.64 m, while the last quad is just a usual FODO quad.

There are 6 straight-section blocks "*BLS*" designed to be used for extraction and injection purposes. There are eight dipoles in each of these blocks. To match this block to the other blocks, the lengths of the first two quads in the low beta insertion cell are slightly different. The first quad is 2.84 m long while the middle one is 4.06 m. The last quad nearest to the low-beta region is the same as a usual FODO quad. There is a 24.1 m available drift for the extraction magnets. Two additional 7.69 meter drifts, designed for the kicker magnets or the electrostatic septa, are located 90° upstream and downstream of the extraction magnet position. The low values of both betatron functions at the extraction magnets in the low-beta insertion imply smaller beam size during the fast extraction. For the slow extraction, it is possible to operate the triplet quads on a different circuit to provide for the necessary high value for one of the betas.

The zero-dispersion straight section is defined within the third block "*BLN*", which is shown in Fig. 3. This block contains 18 dipoles and has a total of a 72 m straight section with zero dispersion. Again, to provide a perfect match to the other blocks the lengths of quads in the low-beta insertion cell are slightly different. The three quads in the triplet have lengths 2.37 m, 4.13 m, and 1.47 m. The zero-dispersion part of the block is designed mostly with FODO cells and is reserved for rf installation.

The blocks are perfectly matched for the β's, α's, and dispersion at the center of the D-quad in the middle of the FODO-cell section, so that the blocks can be shuffled in any order provided that geometric closure is retained. For this design, the arrangement is $2(BLS, BLN, BLS, 6(BLR), BLS, BLR)$. The differences in lengths between the low-beta quads of different blocks may be accommodated with power supply controls, (special shunt supplies on the same bus).

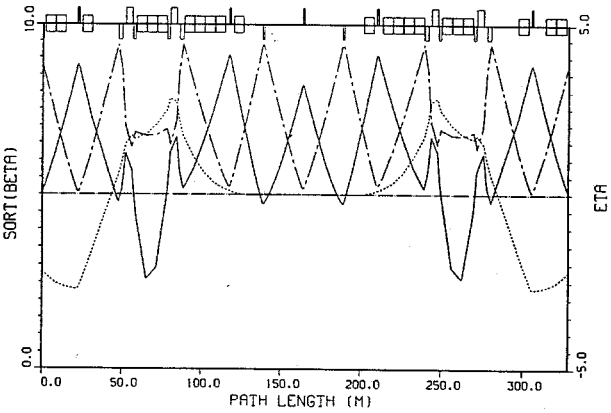

Fig. 3. *The betatron and dispersion functions within the block (BLN) with zero-dispersion straight of the imaginary γ_t lattice.*

IV. Chromaticities and Momentum Dependence

The natural chromaticities of this imaginary γ_t example are $\xi_x = -26.02$ and $\xi_y = -23.95$, of the same magnitude as $|\gamma_t|$. The horizontal and vertical tunes are 19.714 and 14.188, respectively. The chromaticity sextupoles S_F are located at the FODO horizontal focussing quads where the horizontal dispersion has negative values of −2.6 m and $\beta_x = 77.6$ m, while the S_D are at the defocusing quads where the dispersion is −2.2 m and $\beta_y = 75.9$ m. The integrated strength of the sextupoles, at a momentum of 150 GeV/c, to compensate for the natural chromaticities are $k_{sf} = -0.056\text{m}^{-2}$ and $k_{sd} = +0.126\ \text{m}^{-2}$, respectively. These strengths correspond to pole-tip fields of 1.74 and 3.49 kG, respectively, at 150 GeV for sextupoles of length 20 cm and aperture 5 cm in radius. There are only 44 S_F's and 22 S_D's, so they are rather strong and introduce quite large nonlinearities, which must be counteracted by the introduction of a family of harmonic sextupoles in order to achieve a large dynamical aperture. The latter will be studied in a separate paper[5].

The betatron functions dependence on momentum of the chromaticity compensated lattice were examined with two computer programs, SYNCH and TEVLAT. The momentum offsets were introduced in small steps within a range of $\Delta p/p = \pm 2\%$ although the estimated momentum spread in the future Main

Injector should be less than ±0.2%. With the off momentum closed orbit, the maxima of the $\sqrt{\beta_x}$ and $\sqrt{\beta_y}$ (which define the beam size) as plotted in Fig. 4 show very small dependence on momentum. At the maximum momentum offsets of $\Delta p/p = \pm 2\%$, $\sqrt{\beta_x}$ changes by ±0.12% while $\sqrt{\beta_y}$ changes by $+1.6/+0.9\%$.

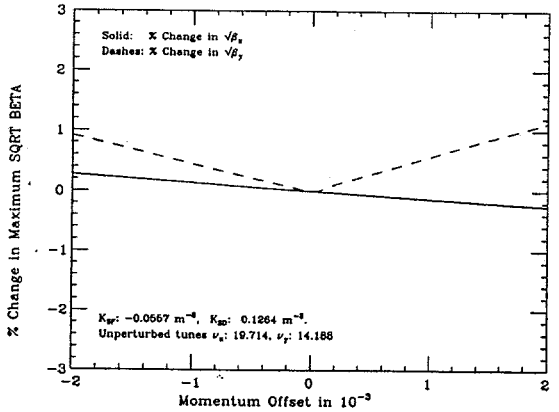

Fig. 4. *A dependence of the maxima of the betatron functions on momentum ($\sqrt{\beta_x}$ and $\sqrt{\beta_y}$).*

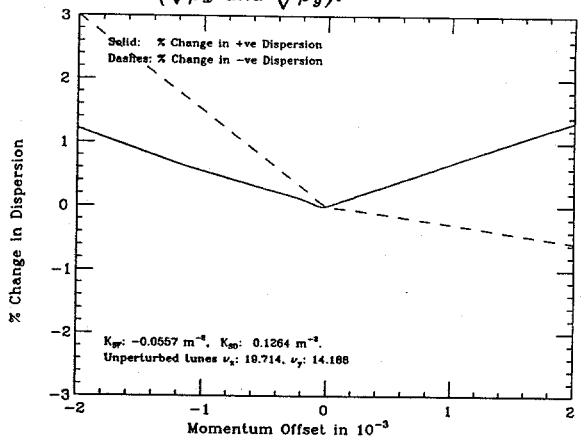

Fig. 5. *The maximum of the horizontal dispersion change on momentum.*

The dispersion function dependence on momentum is presented in Fig. 5. The maximum change of the maxima of the positive horizontal dispersion function at $\Delta p/p = -2\%$ and $\Delta p/p = +2\%$, are $\Delta D_x = +3\%$ and $\Delta D_x = +1.16\%$, respectively. The maximum change of the maxima of the negative dispersion are $\Delta D_x \cong \pm 1.1\%$. for the momentum offsets of $\Delta p/p = \pm 2\%$.

The maximum positive horizontal displacements at the off momentum closed orbit, calculated with SYNCH, are $x^{co}_{max} = 5.6$ mm at both momentum offsets of $\Delta p/p = \pm 2\%$, while the maximum negative horizontal displacements are $x^{co}_{max} = -5.6$ mm. The transition gamma showed a linear dependence on momentum offsets varying from $i23.766$ to $i24.788$ for $\Delta p/p = -2\%$ to $\Delta p/p = +2\%$. With the chromaticity compensated lattice, the tune dependence on momentum showed a parabolic function with a maximum of the horizontal tune shift of $\Delta\nu_x = -0.0001$ and $\Delta\nu_y = -0.00048$ for $\Delta p/p = \pm 2\%$.

V. Conclusion

We have presented a very compact imaginary-γ_t lattice for the Fermilab Main Injector. The whole lattice contains only 220 quads, only ~ 10% more than the usual FODO design. It is important to note that the desired value of the γ_t can be selected easily during the design procedure because the value depends on the average value of the dispersion function through the dipoles. To avoid head-tail instability, one usually need to operate at slight negative (positive) chromaticities below (above) transition. An imaginary-γ_t lattice is always below transition so that no positive-chromaticity operation is necessary. As a result, the correction sextupoles need not be as strong as those in the FODO design.

The momentum acceptance of this imaginary γ_t lattice is very good. The dispersion function propagates through the ring equally between the positive and negative values. The transverse motion of the off momentum particles is especially advantageous, because particles with the higher/lower momenta travel through the dipole magnetic field inside/outside of the central curvature. A displacement of the off momentum particles after the dipole $\Delta x = D\Delta p/p$ in the imaginary γ_t lattice has opposite sign than in the regular FODO cell lattice. With this lattice there is no need for the dipoles with an opposite bend angle[7] to cancel out the longer/shorter path length of the higher/lower momenta particles to avoid transition. In the imaginary γ_t lattice the horizontal offsets and their slopes at the dipoles were designed to provide this cancelation.

The values of the dispersion function with this method are much lower than any previous transitionless design. The betatron functions in all imaginary γ_t lattices designed by this method were within the same range as the corresponding FODO cell lattices or the other imaginary γ_t lattices.

References

[1] K.Y. Ng, *"Some Estimates Concerning Crossing Transition in the Main Injector,"* in *Proc. of the Fermilab III Instabilities Workshop*, Fermilab, June 23-29, 1990, pp. 134-140; S.Y. Lee and K.Y. Ng, *"Longitudinal and Transverse Instabilities around a γ_t Jump," ibib.* pp. 170-176; K. Ng, *"Transverse Emittance Growth during a γ_t Jump," ibib.* pp. 207-212.

[2] James E. Griffin, *"Synchrotron Phase Transition Crossing Using an RF Harmonic,"* Fermilab Internal Memo, March 1991.

[3] T. Risselada, *"Design of Quadrupole Schemes to Modify Gamma Transition,"* Lecture given at *CERN Accelerator School,* KFA Jülisch, 17-28 September, CERN PS/90-51, October 1990.

[4] D. Trbojevic, D. Finley, R. Gerig, and S. Holmes, *"Design Method for High Energy Accelerator without Transition Energy,"* in *Proceedings of the Second European Particle Accelerator Conference,* Nice, France, June 1990, pp. 1536-1538.

[5] K.Y. Ng, D. Trbojevic, and S.Y. Lee, *"Examination of the Stability of the Advanced Imaginary γ_t Lattice,* in these proceedings.

[6] E.D. Courant and H.S. Snyder, *"Theory of the Alternating Gradient Synchrotron,"* Annals of Physics, vol. 3, pp. 1-48, 1958.

[7] G.V.V. Vladimirski and E.K. Tarasov, *Theoretical Problems of the Ring Accelerators,* USSR Academy of Sciences, Moskow, 1955.